GEOCHEMICAL AND GEOMORPHOLOGICAL EFFECTS OF POST-IMPACT HYDROTHERMAL SYSTEMS INCORPORATING FREEZING.

C. J. Barnhart[1], F. Nimmo[1], and B. J. Travis[2] [1]Dept. of Earth and Planetary Sciences, Univ. of California, Santa Cruz, 1156 High St. Santa Cruz, CA 95064 (barnhart@pmc.ucsc.edu), [2]Earth and Environmental Sci. Div., EES-2/MS-F665, LANL, Los Alamos, NM 87545

Summary: Post-impact hydrothermal (PIH) systems subjected to mars-like surface temperatures (-53 °C) and reasonable surface permeabilities (10^{-14} to 10^{-10} m^2) produce flow patterns with spatially diagnostic, surface-exposed water-to-rock (W/R) ratios of ~1 to 1000, channel-carving surface discharge rates of ~1 to 10 m^3/s and lake-forming total discharges of ~10^9 to 10^{12} m^3. A bolide 3.9 km in diameter traveling at 7 km/s generates a 45 km crater and delivers enough energy to heat subsurface water, and drive hydrothermal circulation (figure 1). This PIH circulation can lead to surface discharge of water, and chemical alteration – both are potentially detectable [1,2,3]. Our models differ from previous efforts [4,5,6,7,8] in that we incorporate freezing.

Model: We simulate the evolution of PIH systems using MAGHNUM (cf. [12]). MAGHNUM solves the time-dependent transport of water and heat through a porous medium. It incorporates phase transitions between ice, water and vapor. Given a particular crater size and associated heat sources, two principal dichotomies control PIH behavior: (1) frozen vs unfrozen surface and (2) conductive vs convective heat and fluid transfer.

Results: Discharge rates, total discharge and W/R ratios increase with permeability [13] (figures 2, 3 and 4). Systems with higher permeabilities (10^{-10} m^2) allow convection: rendering them capable of mining heat from the central uplift before the surface freezes. Convective systems subjected to surface temperatures below freezing are particularly interesting because an impermeable freezing front – the surface ice/water interface that marches from mid-floor to the central peak – forces flow towards the center of the crater. This effect prolongs modest near-surface temperatures (0 to 100 ° C for 50 kyr) and yields W/R ratios > 1000. For systems with lower permeability, the upper 200 m of rock at the crater's center experience fluid temperatures between 0 and 100 °C for 3500 yrs and W/R ratios of ~ 10. These results imply that different surface permeabilities should produce spatially diagnostic mineral alteration patterns (figure 3). This may explain mineral assemblages and fluvial features associated with central peaks of craters [3]. Discharge rates and total discharges are capable of producing gullies, ponds and lakes, but not alluvial fans (table 1).

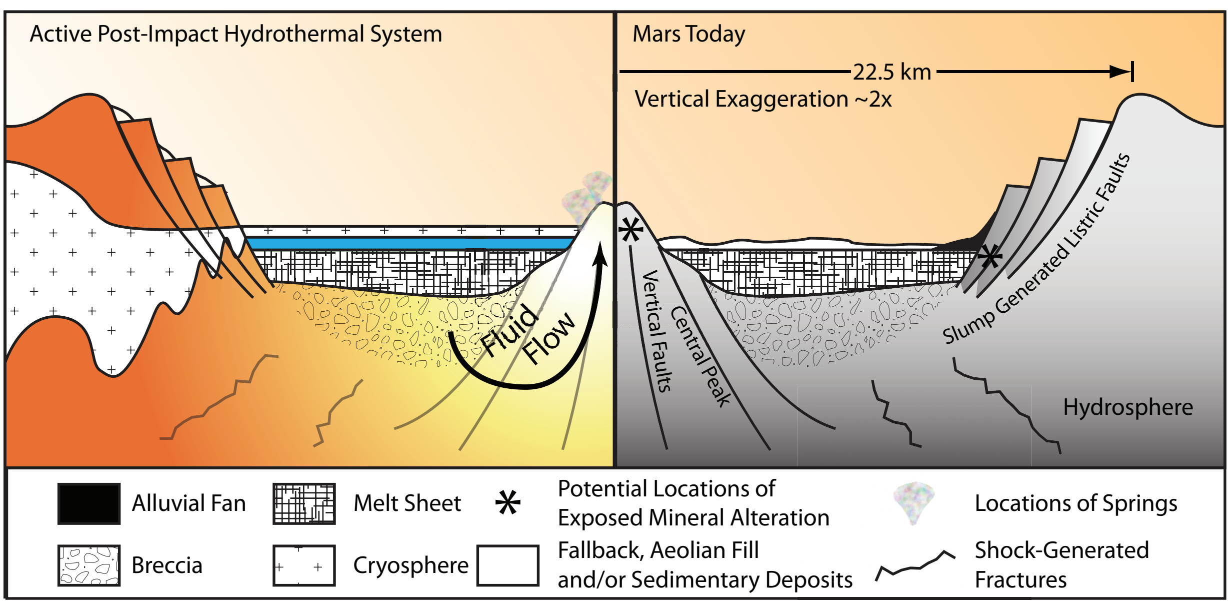

Figure 1: A schematic diagram of an active (left) and fossilized (right) PIH system (*motivated by* [4-11]). The energy delivered by a bolide and the redistribuiton of shock-heated material sets the stage for subsequent hydrothermal activity [*cf. 9,10,11*]. We model PIH systems exposed to clement (5 °C) and subfreezing (- 53 °C) atmospheres in effort to predict their observable effects. Simulations run for 330 kyrs in a 2D axisymmetric domain that spans 30 km radially and 10 km deep (dr = 333 m, dz = 200 m). We assume surface permeabilities of 10^{-10}, 10^{-12}, 10^{-14}, and 10^{-16} m^2 that, along with porosity, decay exponentially with depth. The initial temperature profile used in our simulations exhibits four notable characteristics: a radially decaying shock-heated region, a subsurface field at radius that remains frozen, hot material that is brought from depth as the crater collapses from transient to final form, and a background geothermal profile of 32.5 or 40 mW m^{-2}.

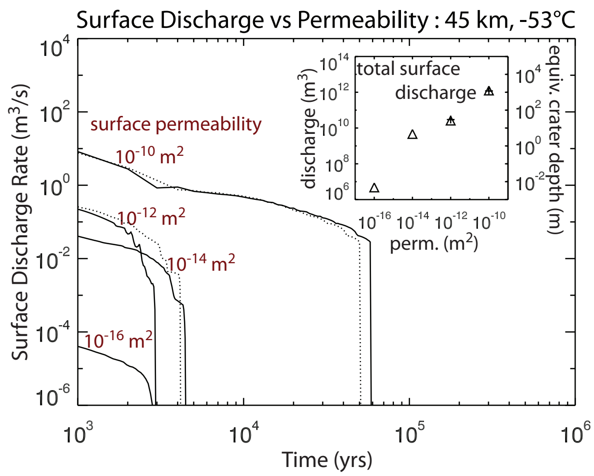

Figure 2: Discharge rate, total discharge, and system lifetime as a function of permeability for PIH systems exposed to a surface temperature of -53 °C. Solid lines and dotted lines indicate a background geothermal flux of 32.5 and 40 mW m^{-2} respectively. The inset shows the equivalent depth that the total discharge would fill a 45 km crater ignoring atmospheric loss. Convective systems (10^{-10} m^2) exhibit prolonged lifetimes and significant surface discharge. Conductive systems (10^{-12} and 10^{-14} m^2) experience a trade-off between system lifetime and discharge rate but produce similar total discharges.

PIH System →	Rate (m^3/s) 1 to 10	Time Active 10^3 to 10^5 yrs	Discharge (m^3) 10^9 to 10^{12}
Outflow Channels	10^4 to 10^9	Uncertain days to yrs	Uncertain 10^{15} to 10^{16}
Valley Networks	10^2 to 10^3	10^3-10^6 yrs episodically	Uncertain 10^{12} to 10^{14}
Alluvial Fans	10^3 to 10^5	< 10^2 yrs	10^{12} to 10^{14}
Gullies	~10 to 30	1-100 days	10^6

Table 1: Discharge rate, periods of activity, and total discharge for Martian fluvial morphologies. PIH system discharge rates are capable of producing gullies but are likely incapable of generating alluvial fans even if permeability structures favored their formation. In all cases a permenantly frozen region prevents discharge near the rim. PIH systems associated with 45 km diameter craters are incapable of supporting valley networks or larger fluvial morphologies. *Values Obtained from*: [15-22]

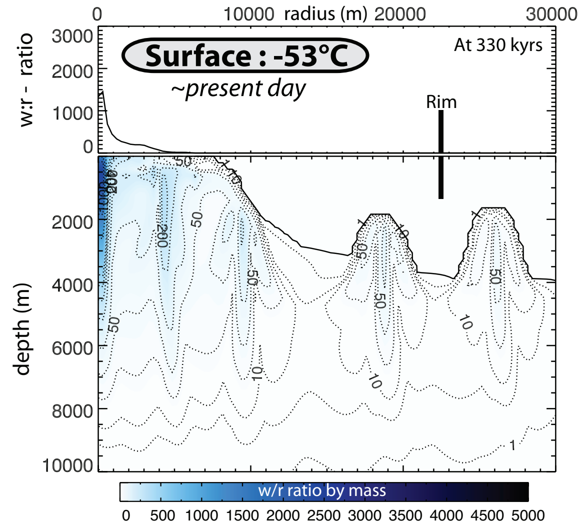

Figure 3: Surface (upper 200 m) W/R ratios as a function of radius for a PIH system with a surface permeability of 10^{-10} m^2 are enhanced at the central peak (top). At depth (contour plot), convective plumes are unable to reach the surface near the rim and do not produce surface discharge there.

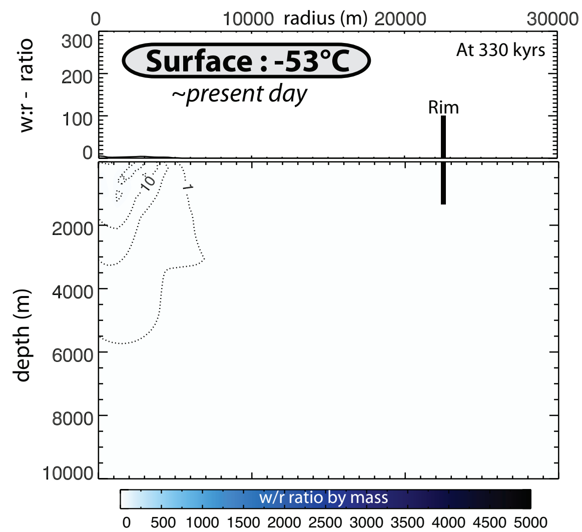

Figure 4: A PIH system with a surface permeability of 10^{-12} m^2 yields low W/R ratios. Low W/R ratios will produce phyllosilicates, chlorites, smectites, mica, amphibole and garnets [2,14]. These clays and minerals are detected in the central peak of a 45 km crater in Nili Fossae [23]. A PIH system with modest surface permeabilities exposed to a frozen atmosphere may have geochemically altered the rock and produced these minerals.

References: [1] Moore J.M. and Howard A.D. (2005) *JGR* 110, E04005. [2] Schwenzer S.P. and Kring D.A. (2008) *LPSC* XXXIX, 1817. [3] Elhman B.L. et al. (2008) *Nat. Geosci.* 1, 355. [4] Newsom H. E. (1980) *Meteoritics*, 15: 339. [5] Newsom H. E. et al. (1996) *JGR*, 101: 14951-14956. [6] Rathbun J. A. and Squyres, S. W. (2002), *Icarus*, 157: 362-372. [7] Abramov O. and Kring, D.A. (2005), *JGR* 110, E9:12. [8] Barnhart C.J. et al., (2008) *LPSC* XXXIX, 2294. [9] Melosh, H.J. (1989), New York, *Oxford Univ. Press*. [10] Davies, G.F. and Arvidson, R.E. (1981) *Icarus*, 45: 339- 346. [11] Shubert, G. and Solomon, S.C. (1992) Mars, *Univ. of Arizona Press*: 147-183. [12] Travis B.J. et al. (2003) *JGR*, 108, E4. [13] Barnhart C.J. et al., (2009) LPSC XXXX, #2013. [14] Schwenzer, S. P. and Kring, D. A., (2009) LPSC XXXX, #1421. [15] Williams, R. M., et al., (2000) *GRL* 27: 1073. [16] Tanaka, K. L. and Chapman, M. G., (1990) *JGR* 95: 14315-14323. [17] Baker, V. R. et al., (1992) Mars, *Univ. of Arizona Press*. [18] Carr, M. H., (1987) *Nature* 326: 30-35. [19] Irwin, R. P., et al., (2005) *JGR* 110 E9. [20] Barnhart, C. J. et al., (2009) *JGR* 114 E13. doi:10.1029/2008JE003122. [21] Kraal, E., et al., (2008) *Nature* 451, 21 doi:10.1038/nature06615. [22] Parsons, R. A. and Nimmo, F. (2009) LPSC XXXX, #1947. [23] Elhmann, B.L., *(submitted to JGR CRISM special issue)*